

Improvement of Thermoelectric Performance in BiCuSeO Oxide by Ho Doping and Band Modulation *

Bo Feng(冯波)^{1,2,3}, Guang-Qiang Li(李光强)^{1,2,3}, Xiao-Ming Hu(胡晓明)^{1,2,3}, Pei-Hai Liu(刘培海)^{1,2,3},
Ru-Song Li(李如松)^{1,2,3}, Yang-Lin Zhang(张阳琳)^{1,2,3}, Ya-Wei Li(李亚伟)^{1,2,3},
Zhu He(贺铸)^{1,2,3}, Xi-An Fan(樊希安)^{1,2,3**}

¹The State Key Laboratory of Refractories and Metallurgy, Wuhan University of Science and Technology, Wuhan 430081

²National-Provincial Joint Engineering Research Center of High Temperature Materials and Lining Technology, Wuhan University of Science and Technology, Wuhan 430081

³Key Laboratory for Ferrous Metallurgy and Resources Utilization of Ministry of Education, Wuhan University of Science and Technology, Wuhan 430081

(Received 1 October 2019)

We try to use Ho doping combined with band modulation to adjust the thermoelectric properties for BiCuSeO. The results show that Ho doping can increase the carrier concentration and increase the electrical conductivity in the whole temperature range. Although Seebeck coefficient decreases due to the increase of carrier concentration, it still keeps relatively high values, especially in the middle and high temperature range. On this basis, the band-modulation sample can maintain relatively higher carrier concentration while maintaining relatively higher mobility, and further improve the electrical transporting performance. In addition, due to the introduction of a large number of interfaces in the band-modulation samples, the phonon scattering is enhanced effectively and the lattice thermal conductivity is reduced. Finally, the maximal power factor (PF) of $5.18 \mu\text{W}\cdot\text{cm}^{-1}\text{K}^{-2}$ and the dimensionless thermoelectric figure of merits (ZT) of 0.81 are obtained from the 10% Ho modulation doped sample at 873 K.

PACS: 72.20.Pa, 72.10.Fk, 74.62.Dh, 72.20.Dp

DOI: 10.1088/0256-307X/37/3/037201

Thermoelectric materials can realize the conversion between thermal energy and electric energy due to the Seebeck effect and the Peltier effect. In the current energy crisis situation, as a kind of clean and energy-saving material, it has attracted much attention and can be used in industrial-waste power generation, refrigeration, thermoelectric catalysis,^[1] and other fields. At present, there are more than 100 kinds of thermoelectric materials, which can be divided into alloy based thermoelectric materials^[2–4] and oxide based thermoelectric materials.^[5–7] The raw materials of oxide based thermoelectric materials are cheap, and they have good oxidation resistance, thermal stability and chemical stability because they themselves contain oxygen. For a long time, the use of oxide based thermoelectric materials has been limited for the low electric conductivity, high thermal conductivity, and the corresponding low conversion efficiencies due to the ionic nature of oxide.^[8,9]

Unlike the previous oxide based thermoelectric materials, the thermal conductivity of BiCuSeO is one order of magnitude lower than traditional oxide based thermoelectric materials.^[10] In addition, the confinement effect of the natural superlattice structure on carriers makes the Seebeck coefficient very high. All these characteristics make it advantageous to possess better thermoelectric performance. The disadvantage is that the intrinsic carrier concentration and mobility are very low, resulting in low electrical conductivity.

Previous studies have mostly focused on composition adjustment. On the one hand, the Bi site could be doped with positive monovalent or positive bivalent elements (Bi showing positive trivalent in BiCuSeO^[11]). According to defect chemistry theory, p-type carrier concentration (holes) can be increased by this way.^[12] On the other hand, the Bi or Te sites could be doped with equivalent elements, according to band theory, which can change the band structure. When the band gap becomes narrower, it is advantageous for the increase of the carrier concentration.^[13,14] When the bandgap becomes wider, it may also be beneficial to the increase of electrical transporting.^[15] In addition, Cu vacancies (Cu shows positive monovalent in BiCuSeO) and Bi vacancies are also used to enhance carrier concentrations.^[16,17] Structural adjustment includes hot pressing to promote the orientations of grains (texturation),^[18] band modulation,^[19,20] and grain refinement. There are few reports on the combination of composition adjustment and structure adjustment. In fact, the materials with better thermoelectric properties are basically based on the combination of the combination.

Here we first dope Bi site with Ho (the same valence as Bi) to adjust the energy band. Ho doping at Bi site as a kind of lanthanide element can be used to adjust the band structure.^[15] In addition, La in lanthanides has been used to improve the thermoelectric properties of BiCuSeO, although the electronegativ-

*Supported by the National Natural Science Foundation of China under Grant No. 51674181.

**Corresponding author. Email: groupfxa@163.com

© 2020 Chinese Physical Society and IOP Publishing Ltd

ity of La (1.10) is smaller than that of Bi (2.02) and O (3.44). That is to say, the electronegativity difference of the $(\text{Bi}_2\text{O}_2)^{2+}$ layer becomes larger when La replaces Bi site, which would enhance the ionicity of the bonds. The electronegativity of Ho (1.23) is higher than that of La, which would make the difference smaller and enhances the covalence of the bonds and correspondingly improve the electrical transporting performance. On the basis of Ho doping, we prepare the band-modulation samples with the same molar amount as the optimum doping amount of Ho by modulating the undoped samples and the heavily doped samples. The advantage of the band modulation is that it is a mixed sample of the undoped sample and the heavily doped sample, the region corresponding to the heavily doped sample is of high carrier concentration and low mobility, while the region corresponding to the undoped sample is of high mobility and low carrier concentration. In the mixed sample, the carriers would preferentially transfer through the region with high mobility, thus helpful for maintaining relatively higher carrier concentration while keeping relatively higher mobility, and correspondingly achieve the effect of improving the electrical transporting performance. In addition, due to the uniform distribution of undoped and heavily doped samples in the mixture-modulated sample, a large number of interfaces would be introduced, which would greatly enhance the phonon scattering and is thus conducive to reducing the lattice thermal conductivity.^[19,21]

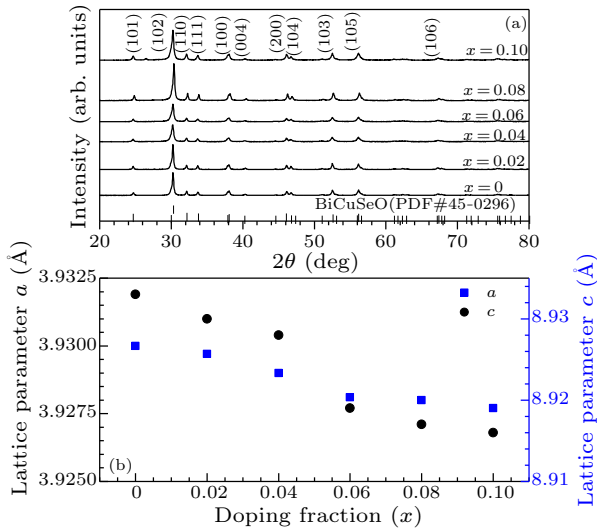


Fig. 1. The XRD patterns (a) and lattice parameters (b) of the BCSO samples

In our experiment, the selected raw materials are as follows: Bi_2O_3 (99.99%), Bi (99.999%), Cu (99.999%), Se (99.99%), Ho_2O_3 (99.99%). Weigh the raw materials according to the stoichiometric ratio of $\text{Bi}_{1-x}\text{Ho}_x\text{CuSeO}$ ($x = 0, 0.02, 0.04, 0.06, 0.08, 0.10$) (called BCSO below), followed by ball milled for 8 hours at 400 r/min under Ar atmosphere, followed by ball milled for 1 hour at 300 r/min with analytical reagent (AR) ethanol absolute ($\geq 99.7\%$). After

drying for 12 hours in a vacuum box, it is sintered (resistance pressing sintering (RPS)) into blocks with the size of $\Phi 20 \times 13$ mm (sintering related details: with argon protection, insulation temperature at 873 K, holding time of 10 min, holding pressure during heat preservation process of 50 MPa).

We chose the undoped BiCuSeO and Ho heavily doped BiCuSeO ($\text{Bi}_{0.80}\text{Ho}_{0.20}\text{CuSeO}$) to prepare the band-modulation samples. The powders of two samples were ball milled for 10 min (at a mole ratio of 1:1), and then sintered by RPS, and the blocks were obtained (the specific sintering parameters were the same as above).^[17] Characterization methods and specific equipment information are described in the previous literature.^[13]

The phases of Ho doped samples were detected by XRD, and the results are shown in Fig. 1(a). It can be seen that the diffraction peaks of all the samples correspond to the standard card of BiCuSeO one by one, and no miscellaneous peaks are found. In addition, in order to analyze the lattice, we have refined the XRD data to obtain the lattice constants, as shown in Fig. 1(b). It can be seen that the lattice constants a and c both show a slight downward trend with the increase of Ho doping amount. The lattice shrinkage is supposed to be caused by the smaller ionic radius of Ho^{3+} (0.901 Å) than that of Bi^{3+} (1.030 Å).^[22]

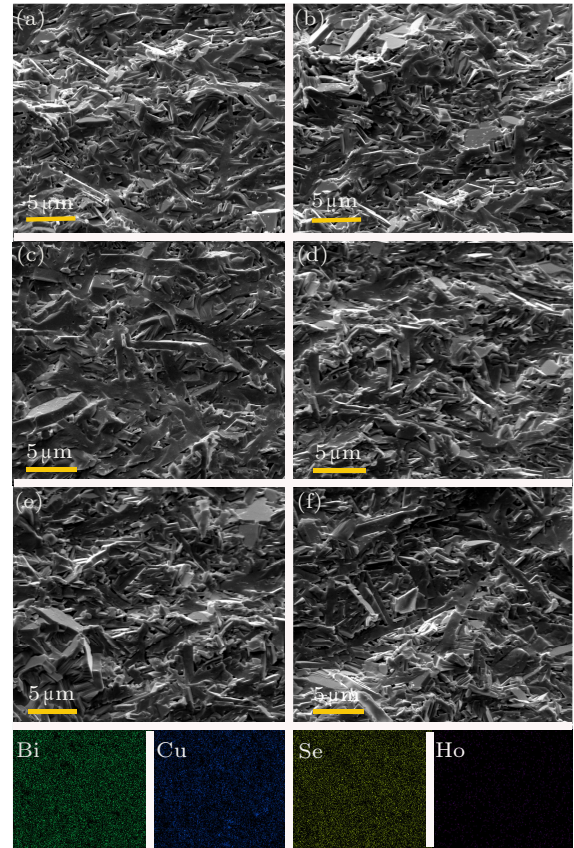


Fig. 2. The fracture morphology of the BCSO samples: (a) $x = 0$, (b) $x = 0.02$, (c) $x = 0.04$, (d) $x = 0.06$, (e) $x = 0.08$, (f) $x = 0.10$, and the EDS results for $x = 0.10$.

Figure 2 shows the fracture morphology of the

BCSO samples. The grain size of the sample is lath and compact. The relative densities of the samples are over 97% as shown in Table 1. With the addition of Ho, the grain size and morphology have no obvious

change. Moreover, the EDS results indicate that all the elements are evenly distributed without obvious segregation.

Table 1. The relative density r , carrier concentration n , mobility μ and the effective mass at Fermi level (m^*) for the BCSO samples at room temperature (m_0 : electronic mass, HD: the heavily doped sample, MD: the modulation doped sample).

Sample	r (%)	S ($\mu\text{V}\cdot\text{K}^{-1}$)	n (10^{19}cm^{-3})	μ ($\text{cm}^2\text{V}^{-1}\text{s}^{-1}$)	m^*/m_0
$x = 0$	97.3	381	1.21	9.12	0.98
$x = 0.02$	97.2	209	1.62	7.59	0.65
$x = 0.04$	99.1	200	3.69	7.23	1.09
$x = 0.06$	98.6	140	5.10	3.88	0.94
$x = 0.08$	98.4	120	6.23	3.56	0.92
$x = 0.10$	97.9	121	6.79	3.65	0.99
HD	97.7	64	10.23	0.45	0.68
MD	98.2	99	7.88	3.72	0.89

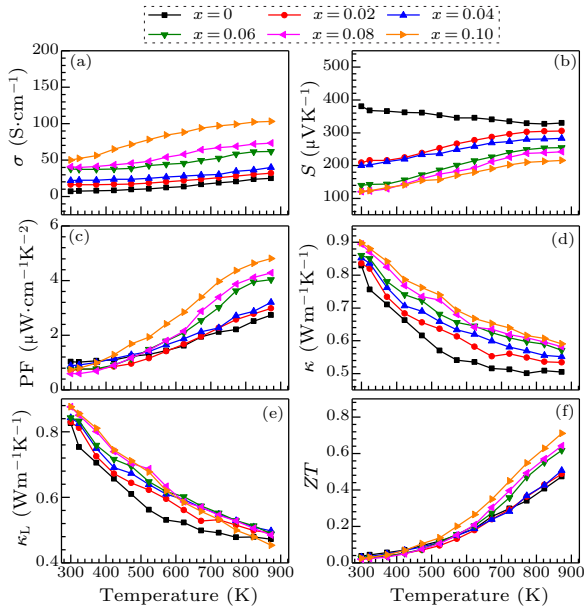


Fig. 3. Temperature dependence of (a) electrical conductivity σ , (b) Seebeck coefficient S , (c) power factor (PF), (d) thermal conductivity κ , (e) lattice thermal conductivity κ_L , and (f) dimensionless thermoelectric figure of merit (ZT) of BCSO.

The electrical conductivity (σ) of the doped sample varies from room temperature to 873 K as shown in Fig. 3(a). With the increase of Ho doping content from 2% to 10%, the electrical conductivity increases in the whole temperature range. The electrical conductivity is determined by the carrier concentration n and mobility μ ($\sigma = n\mu e$ with e being the carrier charge). To analyze the reason why the conductivity increases with the increase of Ho doping content, Hall test was carried out, and the results are listed in Table 1. It can be seen that n increases with the increase of doping content, from $\sim 1.21 \times 10^{19} \text{ cm}^{-3}$ of the undoped sample to $\sim 6.79 \times 10^{19} \text{ cm}^{-3}$ of the 10% Ho doped sample. At the same time, μ declines slightly. The increase of conductivity should be due to the increase of n .

The Seebeck coefficient S of the doped sample varies from room temperature to 873 K as shown in Fig. 3(b). With the increase of doping amount, S shows a downward trend. This should be due to the

increase of n , which is negatively correlated with the Seebeck coefficient expressed as^[23]

$$S = \frac{8\pi^2 k_B^2 T}{3eh^2} m^* \left(\frac{\pi}{3n} \right)^{2/3} \quad (1)$$

Figure 3(c) shows the relationship between the power factor (PF) and temperature for the BCSO samples. Because the Seebeck coefficient decreases slightly in the low temperature range (just above room temperature in the thermoelectric community), the PF has no obvious advantage in the low temperature range, even lower than the undoped sample, whereas it increases greatly in the middle and high temperature range. The highest PF of $4.81 \mu\text{W}\cdot\text{cm}^{-1}\text{K}^{-2}$ was obtained at 873 K for the 10% Ho-doped sample, which is 1.73 times the undoped one.

The total thermal conductivity (κ) of the doped sample varies from room temperature to 873 K as shown in Fig. 3(d). It can be seen that κ decreases with the increase of temperature in the whole temperature range, which is due to the enhancement of phonon scattering and the corresponding decrease of lattice thermal conductivity (κ_L) ($\kappa = \kappa_L + \kappa_E$, with κ_E being the electronic thermal conductivity). In addition, with the increase of Ho doping amount, κ increases in the whole temperature range. On the one hand, because σ increases in the whole temperature range, the corresponding κ_E increases in the whole temperature range ($\kappa_E = L\sigma T$, L is the Lorenz number). On the other hand, although the heterostructure scattering caused by doping contributes to the enhancement of phonon scattering to decrease κ_L . However, it should be noted that Bi (209), as a heavy element, is one of the reasons for the low lattice thermal conductivity of BiCuSeO. Ho (165) is lighter than Bi, which would cause higher sound velocity, higher lattice vibration frequency and corresponding higher lattice thermal conductivity,^[24] as shown in Fig. 3(e).

The dimensionless thermoelectric figure of merit (ZT) of the doped sample varies from room temperature to 873 K as shown in Fig. 3(f). Because the PF has no obvious advantage in the low temperature range (just above the room temperature in the ther-

moelectric community) and the thermal conductivity increases in the whole temperature range, the advantage of ZT in the low temperature range is not obvious, but ZT increases significantly upon Ho doping in the medium and high temperature range. The highest ZT value of 0.71 was obtained from the 10% doped sample at 873 K.

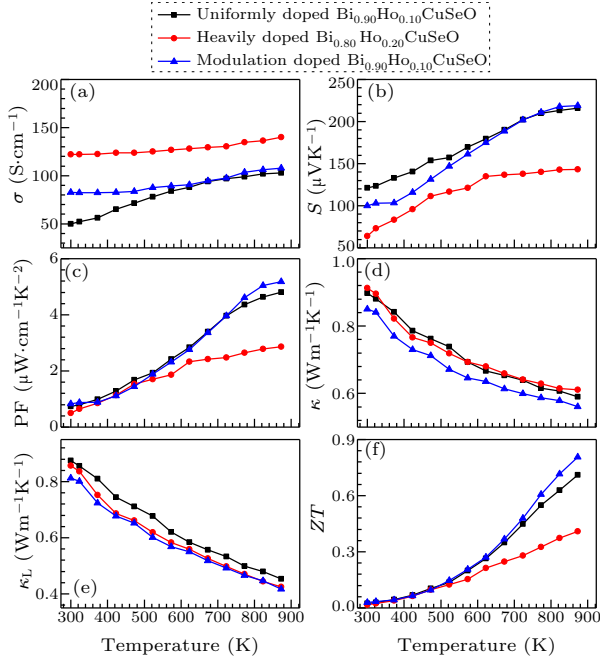


Fig. 4. Temperature dependence of (a) electrical conductivity σ , (b) Seebeck coefficient S , (c) power factor (PF), (d) thermal conductivity κ , (e) lattice thermal conductivity κ_L , and (f) ZT values of the uniformly doped/heavily doped/modulation doped BCSO.

Figure 4(a) shows the relationship between the electrical conductivity σ and temperature for the uniformly doped (UD) $\text{Bi}_{0.90}\text{Ho}_{0.10}\text{CuSeO}$, the heavily doped (HD) $\text{Bi}_{0.80}\text{Ho}_{0.20}\text{CuSeO}$, and the band-modulation doped (MD) $\text{Bi}_{0.90}\text{Ho}_{0.10}\text{CuSeO}$. It can be seen that σ of the HD sample is further improved, while that of the MD sample, with the same molar amount as the UD sample, is higher than that of the UD sample. The corresponding Hall test results are listed in Table 1. It can be seen that the reason for the increase of σ is that the n and μ of the MD sample are both higher than those of the UD sample. The reason lies in the special characteristics of the mixture structure of band-modulation samples. In the heavily doped sample region, n is high and μ is low. In the undoped sample region, n is low and μ is high. For the mixed structure of the MD sample, the carriers will preferentially pass through the region with high mobility, as shown in Fig. 5, thus maintaining high mobility while maintaining high carrier concentration, and correspondingly improving the electrical transporting performance.^[19,20]

Figure 4(b) shows the relationship between the Seebeck coefficient S and temperature for the band-modulation related samples. It can be seen that the S

of the HD sample is lower than UD in the whole temperature range, which is due to the increase of n . The S of the MD sample is lower than UD in the low-mid temperature range because of the increase of n , but almost the same as or even more than that of the UD sample in the high temperature range.

From Fig. 4(c), it can be seen that PF of the HD sample decreases in the whole temperature range because the increase of σ cannot compensate for the decrease of S . The PF of the MD sample is not so far different from that of the UD sample in low-mid temperature range, but higher in high temperature range, reaching the highest value of $5.18 \mu\text{W}\cdot\text{cm}^{-1}\text{K}^{-2}$ at 873 K.

It can be seen from Fig. 4(d) that the κ of the HD sample has little difference with UD sample in the whole temperature range due to the offset of the decrease of κ_L and the increase of κ_E . Although κ_E in MD sample is higher than that of UD sample due to the increase of σ , κ is lower than that of the UD sample in the whole temperature range due to the sharp decrease of κ_L as shown in Fig. 4(e). The reason why the κ_L of the MD samples decreases is that the band-modulation mixture of undoped samples/heavily doped samples introduces amount of interfaces, which could enhance the scattering of phonons.

Figure 4(f) shows the relationship between the dimensionless thermoelectric figure of merits (ZT) and temperature for the uniformly doped (UD) $\text{Bi}_{0.90}\text{Ho}_{0.10}\text{CuSeO}$, the heavily doped (HD) $\text{Bi}_{0.80}\text{Ho}_{0.20}\text{CuSeO}$, and the band-modulation doped (MD) $\text{Bi}_{0.90}\text{Ho}_{0.10}\text{CuSeO}$. As the PF decreases in the whole temperature range, the ZT of the HD sample decreases in the whole temperature range. Because of the decrease of κ , the ZT value of the MD sample increases, especially in the high temperature range, reaching the highest value of 0.81.

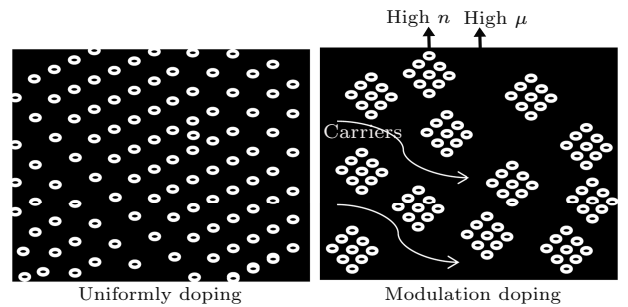


Fig. 5. Schematic diagrams for the carrier transporting of the uniformly doped $\text{Bi}_{0.90}\text{Ho}_{0.10}\text{CuSeO}$ and the modulation doped $\text{Bi}_{0.90}\text{Ho}_{0.10}\text{CuSeO}$ samples.

We aim to improve the thermoelectric performances of BiCuSeO by Ho doping and band modulation. The corresponding samples are prepared by ball milling combined with RPS. The experimental results show that Ho doping can increase the carrier concentration effectively, thus effectively enhances the electrical conductivity. The power factor is effectively enhanced in the middle and high temperature range.

Although the thermal conductivity is increased due to the increase of carrier thermal conductivity and lattice thermal conductivity, the ZT value is still increased, especially in mid-high temperature range. The band modulation based on this can increase the carrier concentration while maintaining high mobility, thus effectively enhancing the electrical conductivity and power factor. In addition, the introduction of the interface leads to a decrease in the lattice thermal conductivity. In this way, ZT is enhanced with a maximum value of 0.81, which is 1.72 times the value of BiCuSeO.

References

- [1] Achour A, Kan C, Reece M J and Huang Z 2018 *Adv. Energy Mater.* **8** 1701430
- [2] Tang X, Xie W, Li H, Zhao W Y and Zhang Q J 2007 *Appl. Phys. Lett.* **90** 012102
- [3] Heremans J P, Jovovic V, Toberer E S, Saramat A, Kurosaki K, Charoenphakdee A, Yamanaka S and Snyder J F 2008 *Science* **321** 554
- [4] Yu T, Decong Land Zhong Chen 2018 *Chin. Phys. B* **27** 118105
- [5] Flahaut D, Mihara T, Funahashi R, Nabeshima N, Lee K H, Ohta K and Koumoto K 2006 *J. Appl. Phys.* **100** 084911
- [6] Ohtaki M, Tsubota T, Eguchi K, Koichi E and Hiromichi A 1996 *J. Appl. Phys.* **79** 1816
- [7] Da Q L, Yu W Z and Hui J K 2018 *Chin. Phys. B* **27** 047205
- [8] Li G J, Zhao S J, Mei A and Lan J 2009 *Adv. Mater. Res.* **79** 2143
- [9] Li J, Sui J, Pei Y, Meng X F, David B, Nita D, Cai W and Zhao L D 2014 *J. Mater. Chem. A* **2** 4903
- [10] Zhao L D, He J, Berardan D, Lin Y H, Li J F, Nan C W and Nita D 2014 *Energy & Environ. Sci.* **7** 2900
- [11] Hsiao C L and Qi X 2016 *Acta Mater.* **102** 88
- [12] Li J, Sui J, Pei Y, David B, Nita D and Zhao L D 2012 *Energy & Environ. Sci.* **5** 8543
- [13] Feng B, Li G Q, Hou Y H, Cheng C Z, Jiang C P, Hu J, Xiang Q S and Fan X A 2017 *J. Alloys Compd.* **712** 386
- [14] Liu Y, Lan J and Xu W 2013 *Chem. Commun.* **49** 8075
- [15] Liu Y, Ding J, Xu B, Lan J, Zheng Y H, Zhan B, Zhang B P, Lin Y H and Nan C W 2015 *Appl. Phys. Lett.* **106** 233903
- [16] Li Z, Xiao C, Fan S, Deng Y, Zhang W, Ye B and Xie Y 2015 *J. Am. Chem. Soc.* **137** 6587
- [17] Liu Y, Zhao L D and Liu Y 2011 *J. Am. Chem. Soc.* **133** 20112
- [18] Sui J, Li J, He J, Pei Y L, David B, Wu H J, Nita D, Cai W and Zhao L D 2013 *Energy & Environ. Sci.* **6** 2916
- [19] Pei Y L, Wu H and Wu D 2014 *J. Am. Chem. Soc.* **136** 13902
- [20] Bo F, Guangqiang L, Zhao P, Jiang C P, Hu J, Xiang Q S and Fan X A 2018 *J. Solid State Chem.* **266** 297
- [21] Dingle R, Störmer H L and Gossard A C 1978 *Appl. Phys. Lett.* **33** 665
- [22] Hmood A, Kadhim A and Hassan H A 2012 *J. Alloys Compd.* **520** 1
- [23] Yang Y, Liu X and Liang X 2017 *Dalton Trans.* **46** 2510
- [24] Lin H, Chen H, Ma N, Zheng Y J, Shen J N, Yu J S, Xu X T and Wu L M 2017 *Inorg. Chem. Front.* **4** 1273